Smart Distributed Energy Storage Controller (smartDESC)

Smart Distributed Energy Storage Controller (smartDESC)

F. Malandra[1,*], A.C. Kizilkale[2], F. Sirois[3], B. Sansò[3], M.F. Anjos[4,3], M. Bernier[3], M. Gendreau[3], R.P. Malhamé[3]

Abstract

While the storage properties and the anticipation potential of many classes of power system loads (such as thermal loads) can be exploited to mitigate renewable sources variability, the challenge to do so in an optimal and coherent manner is significant. This is due to the sheer number and dynamic diversity of the loads that can be involved in any large-scale application. The smartDESC concept is a control architecture that was developed for this purpose. It builds on the more pervasive communication means currently available (such as Advanced Metering Infrastructures), as well as the mathematical tools of (i) aggregate load modeling, (ii) renewable energy forecasting, (iii) optimization theory, deterministic or stochastic, and (iv) some recent developments in control of large-scale systems based on game theory, and so-called mean-field (MF) control theory, which allow a scalable yet optimal approach to the decentralized control of large pools of loads. This paper presents the building blocks of the smartDESC architecture, together with an associated simulator and simulation results.

Abbreviations

AMI	Advanced Metering Infrastructure
EWH	Electric Water Heater
MF	Mean Field
smartDESC	Smart Distributed Energy Storage Controller
s-EWH	smartDESC controlled EWH
t-EWH	Thermostatically controlled EWH

1. Introduction

1.1. Motivations behind this work

Increasing the share of renewable energy sources in worldwide energy production is an unanimously recognized objective. The main challenge in integrating most renewable energy sources, such as from sun, wind, and tides, in power systems resides in their intermittent nature, as there is no guarantee that the power required by consumption centres can be exclusively provided by such energy sources at any given time, unless large-scale energy storage facilities can be made available to defer the use of renewable energy in time.

It is also well known that grid-scale energy storage for electric power is difficult to justify from an economic standpoint. One approach to circumvent this difficulty is to use the existing storage potential in customer premises, such as electric water heaters or even the energy stored in the thermal mass of buildings (from furnitures, walls, etc.) [1]. Nevertheless, such an approach is not easily scalable as the number of storage sites to control grows very quickly. Therefore, in order to maximise the potential of this storage, new types of control architectures must be developed. The challenge is even harder if the storage management is required to be completely transparent in terms of customer comfort.

The main objective of the smartDESC concept, summarized in this paper, is precisely to fulfil this emerging need of a distributed storage mechanism to i) increase the penetration of energy from renewable sources, and ii)

*Corresponding author
[1]University at Buffalo, Department of Electrical Engineering, Buffalo, NY, U.S.A.
[2]Automat.AI, Montreal, QC, Canada.
[3]Polytechnique Montreal, Montreal, QC, Canada.
[4]University of Edinburgh, School of Mathematics, Edinburgh, Scotland.

smooth power consumption peaks that are particularly difficult to manage by the power operator. smartDESC is based on a decentralized control scheme that can be scaled up to millions of controlled loads with minimal customer discomfort, and without overloading the telecommunication infrastructure, as commonly happens with centralized controllers.

1.2. Background

Since the 1970s, direct control of consumers' load, usually called "demand response", has been considered a tool to shape the global electric consumption profile in power systems to achieve peak load shaving and valley filling [2, 3]. Such measures allow deferring installation of new generation equipment and using generators near their most efficient operating point. However, large-scale deployment of demand response strategies has only been seriously considered with the increased penetration of intermittent renewable energy sources [4–10]. Indeed, the generation variability and diminished predictability caused by the presence of renewables put pressure on the ability of independent system operators to maintain grid stability and ensure reliable power delivery [11, 12].

Demand response is one of the numerous functionalities expected from the power systems of the future, commonly referred to as "smart grids". One of the key features of smart grids is their ability to rely on an increasingly pervasive communication network, which is intended to allow a progressive sharing of the responsibility of balancing the electricity demand with the power generation between the producers and the consumers. The role of consumers is indeed gradually changing in that they can now contribute to power generation, mostly through rooftop solar panels, electric batteries in dwellings or electric vehicles [13–17]. This rapidly changing electric grid landscape has produced both a need to anticipate the new dynamics via adequate modeling tools, and a need to develop new control frameworks capable of handling a very large number of heterogeneous control points and the presence of a large number of agents or decision makers.

In this context, ideas of hierarchical control architectures are beginning to emerge, such as smartDESC, described for the first time in this paper. On top of any hierarchical control architecture, there is a "coordinator" [18, 19] that can either be the power system operator or a third party called "aggregator", who enlists the commitment of a large pool of customer loads by means of financial incentives. The loads must be coordinated so as to deliver an aggregate load behavior which is desirable from the power system point of view.

The key to scalability in hierarchical control architectures is that the coordinator must work with a collection of low-order macro models of the various homogeneous load subclasses in order to identify optimal feasible aggregate load behaviors at a reasonable computational cost. These global requirements must subsequently translate into microscopic individual load control actions. In [18, 19], the microscopic control actions are centrally dictated. By contrast, in [20], the devices switch on or off probabilistically, according to a coordinator signal strength, and convergence to aggregate objectives is achieved via both control and reliance on the law of large numbers. The approach used in smartDESC is closer to [20], except that in producing the microscopic device-wise actions to attain the global objectives, the recent theory of Mean Field (MF) control theory [21] is applied. Devices are attributed an individual cost function which encapsulates conflicting objectives: local customer comfort and safety, but with compulsory global objectives enforced on the mean behavior of the population of devices [22, 23].

1.3. Contributions and paper organization

The main contribution of smartDESC is to provide an original scalable hierarchal controller architecture based on the state-of-the-art mean-field control theory. smartDESC's architecture also includes a computation and communication framework that allows turning a large pool of consumers' energy-storing loads into a virtual battery under the control of a single *aggregator*. While in our presentation, the *aggregator* is considered to be the power system operator, the proposed architecture could work equally well for a third-party entity offering load dispatch services on the energy market. The focus of the analysis is on Electric Water Heater (EWH) loads, but other types of loads can be easily integrated.

The architecture of the smartDESC controller is shown in Figure 1. At the top left sits a *coordinator*: its function is to produce piecewise-constant "optimal" targets for the mean energy content per device in the aggregate, or equivalently, mean water temperature, over successive 30-minute periods. At the top right, a node represents the renewable generation forecast. At the bottom of the figure, we can find the collection of controlled devices (here the EWHs). In the smartDESC architecture, EWHs must collectively meet the dictated aggregate mean energy targets (i) with minimal information exchange with the *coordinator* (decentralization), (ii) with no impact on users' comfort, and (iii) while keeping the devices in their safe zone of operation. In the middle, we can observe the *communication* module, which permits the required data exchange at a low but sufficient rate to ensure proper operation.

The paper describes in details the main features of each smartDESC module, namely the *coordinator* module, the *communication* module and the *controller* module. Then, a dedicated section presents the smartDESC "simulator", which has been an essential tool to develop and test the concepts behind the project, and which was used to generate proof-of-concept results, which are presented in the last part of the paper.

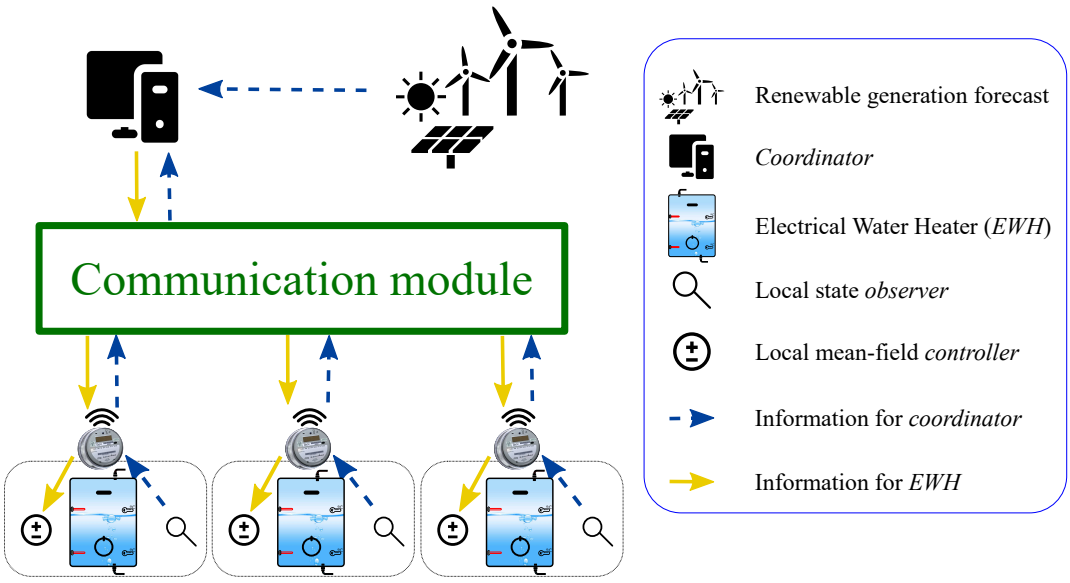

Figure 1: Architecture of the smartDESC concept.

2. The *coordinator* module

In order to enable the desired optimization function of the *coordinator*, i.e., that of coordinating devices to help mitigate the generation variability due to intermittency of the renewable energy sources, two conditions must be met: the *coordinator* must have a reasonably reliable, yet sufficiently simple model of the aggregate storage potential of the EWHs; (ii) the *coordinator* must be fed with forecasts of the renewable energy to be expected over the next 24 hours.

To comply with the first condition, a large EWH with water mass equal to the total water mass in the aggregated devices is used for each homogeneous sub-population of devices. In addition, while the heating element power in the aggregated device is bounded above by the sum of maximal heating powers, and below by zero, in practice, only a subset of that range can be achieved by the aggregate. This range will depend on the current temperature distribution within the devices. An algorithm going back and forth between aggregate modeling, optimization, the *coordinator* module, and simulation of impact on devices is developed to correctly estimate the maximal and minimal heating rate bounds [24]; finally, the physical parameters of the aggregated smartDESC, including inlet water temperature, heat loss rates, and overall water extraction statistics in the controlled pool of devices must be periodically updated.

All the above functions must be performed by a *data analysis* sub-module within the *coordinator* module, as shown in Figure 2. Based on the above information, the *coordinator* module calls the *optimization* sub-module, which performs a deterministic or stochastic optimization over an adequately chosen time horizon. The *optimization* sub-module also generates the optimal feasible mean target temperature profile for each homogeneous subgroup of EWHs. The *optimization* module can perform deterministic or stochastic optimization. In the former, classical peak shaving objectives are employed whereas, in the latter, forecasts on the renewable generation are considered. The optimization problem must be solved quickly enough to react, at least in part, to unpredicted changes relative to any of the forecast quantities (the spinning reserves being the ultimate line of defense against the thoroughly intractable components of this variability). Additional details on the *optimization* sub-module can be found in [25, 26]. Ultimately, the 24-hour mean temperature profile targets for each homogeneous sub-group of controlled EWHs, together with the associated initial mean water temperatures, are transmitted to the *communication* module to be broadcast to the corresponding sub-groups of devices.

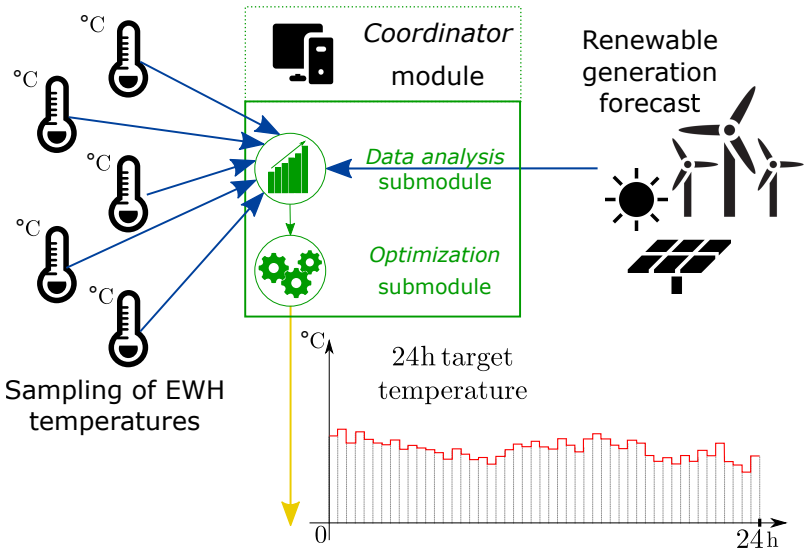

Figure 2: Schematic of the *coordinator* module.

3. The *communication* module

Telecommunications play a key role in every smart grid application: the bidirectional flow of information is a key component for intelligence in smart grids. It is therefore important to accurately model data flow in the smartDESC network. The implementation of the *communication* module is depicted in Figure 3. In the top left, there is a simplified architecture of the proposed smartDESC simulator with one *coordinator* and 3 EWHs. As can be seen, each EWH is composed of a local state *observer*, a local *MF controller* and a *smart meter*, which is used to wirelessly transmit/receive the smartDESC packets.

Two types of communication are required: (i) downlink, from the *coordinator* to all the local *MF controllers* of the collection of devices; (ii) uplink, in the opposite direction (see Figure 3). The *communication* module handles the transmission of 2-way information between the *coordinator* module and the collection of devices in a timely manner. The uplink direction is represented in Figure 3 by dashed blue arrows, while the downlink direction is represented in the same figure by solid yellow arrows.

The *coordinator* needs to periodically send the target mean temperatures to all local *MF controllers* as segregated into homogeneous sub-groups. Also, it must provide to each sub-group updated information on the mean temperature of the subgroup at the beginning of each control period. Based on this information, the MF optimal state feedback policy for the particular sub-group to which an EWH belongs is locally calculated and locally applied to each device *as long as it does not violate predefined comfort and safety constraints*. In addition, in order to generate an anonymized temperature distribution estimation of the whole EWH population, each *MF controller* sends back to the *coordinator*, at low frequency and randomly distributed times, its current mean temperature with a time stamp; a monthly update of the EWH local water draw statistical model is also sent back to the *coordinator*. The overall data is consolidated at the level of the *data analysis* sub-module of the *coordinator* to maintain updated versions of aggregated models.

The overall exchange rate of information is very low (on average below 10 messages per day per EWH) and the packet size is very small (in the order of a few hundred bytes). Among the available communication architectures, it was proposed to use a particular type of Advanced Metering Infrastructure (AMI) that uses unlicensed radio frequencies to create a mesh topology between the smart meters and the power utility Metering Data Management System. This architecture is called RF-mesh and was originally deployed to remotely read residential and commercial power meters, but it is also suitable for applications without high communication requirements, such as those of smartDESC. The RF-mesh system is a middle layer that allows the communication between the local *MF controllers* and the *coordinator*. It is important to remark that the proposed mesh topology provides reliable and redundant communication paths for the bidirectional flow of smartDESC packets. Smart meters are densely present in urban environments and they actively contribute to the dissemination of packets [27]. Furthermore, in rural areas, where the smart meters are less densely deployed, wireless routers are installed to increase coverage and enhance connectivity. The chosen configuration is robust and densely connected (especially in urban areas), thanks to the large number of alternative paths available among data collectors and smart meters. Therefore, this

topology permits to resist to temporary node and link failures.

To prove the concept before suggesting a field deployment, a dedicated *communication* module was implemented and integrated into a smartDESC simulator. The role of the *communication* module is to model the network delay introduced by the RF-mesh system. Further details can be found in [27–30].

In the lower part of Figure 3, a representation of the RF-Mesh network is depicted. As shown in this figure, the smart meters included in the smartDESC architecture represent only a fraction of all the smart meters simulated in the RF-Mesh *communication* module: this is due to the fact that the number of smart meters in a typical RF-Mesh system exceeds the number of EWHs analyzed in smartDESC. Even though a large number of smart meters included in the *communication* module are not used to carry smartDESC data, they are important to accurately model a realistic RF-Mesh system and to obtain meaningful results on network performance (e.g., collision probability, resource utilization, and delay).

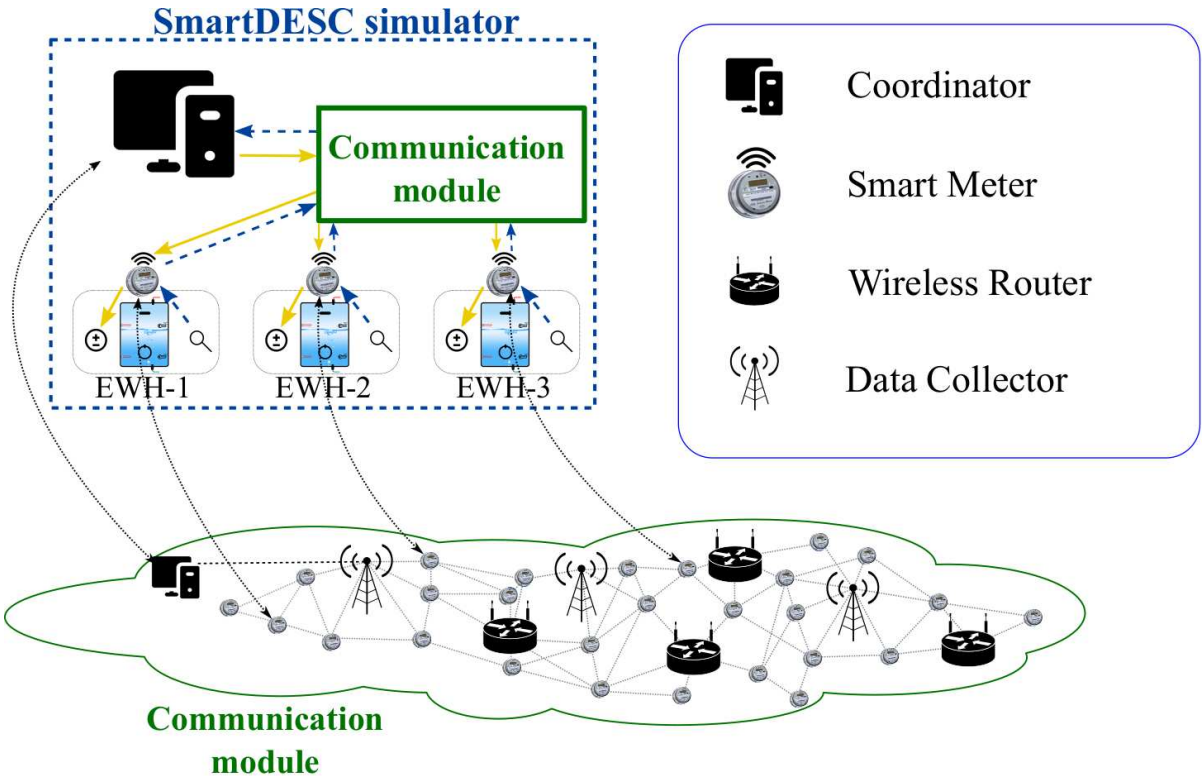

Figure 3: Schematic of the *communication* module.

4. The local *controller*

Upon receiving a mean target temperature signal from the *coordinator* module, which is specific to its particular homogeneous subgroup, the local *MF controller* must synthesize a local state feedback heating control law consistent with that signal. While the control law is common to the whole sub-group, it is locally computed so as to minimize the overall communications requirements of the architecture. This computation is enabled by a sequence of building blocks, as shown in the schematic in Figure 4: (i) an EWH stochastic state space model: it characterizes the internal dynamics of the EWH when subjected to random hot water extraction processes; (ii) a local state *observer*: it is needed because the EWH energy state, including in particular the binary hot water demand component of the state vector, cannot be directly measured, but must rather be inferred from a reduced set of measurements performed on the device; (iii) a local *MF controller*: it is the heart of the computation leading to an EWH control law which, while applied based on local information only, leads to a collective behavior of the homogeneous sub-group *consistent* with the targets dictated by the *coordinator*. We now provide further details on these building blocks.

4.1. EWH stochastic state space model

There is a trade-off between the modeling accuracy of EWHs and the simplicity of calculating aggregate dynamics for a large population. First of all, it is not surprising that the actual temperature dynamics in an EWH tank,

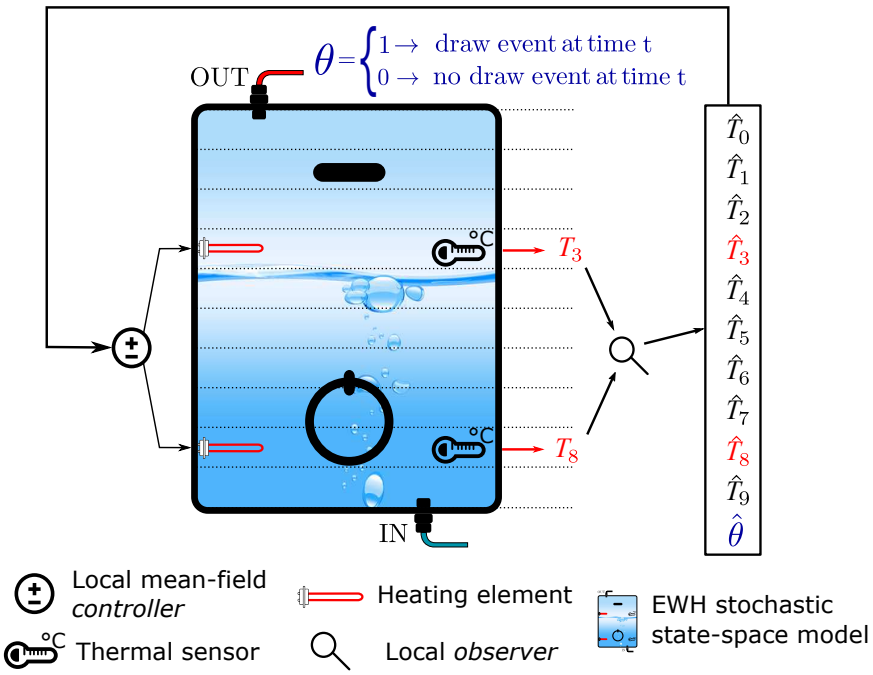

Figure 4: Schematic of the local *controller* of an EWH.

which is subject to thermal stratification, is nonlinear. However, aggregation of nonlinear dynamics poses further complexity on the optimization module as well as for local control synthesis; therefore, a linear model is adopted. After some adjustments to reflect the nonlinear convection effects , the linear model has been observed to provide acceptable accuracy in comparison with simulations performed with TRNSYS[5], a widely accepted thermal system simulation program. Linearity in dynamics is a key component for this work. The linear model is depicted in Figure 4. In this specific case, there are 10 water stratification layers, one local *MF controller* connected to two heating elements, and one local *observer* module, which receives the temperature from two sensors. Cold water flows from the bottom layer to the top layer when water draw events occur. Furthermore, the statistics of hot water extraction events are modeled as a binary state Markov chain with switching rates that vary depending on the hour of the day [31].

4.2. Local state observer

As seen in Figure 4, the thermal dynamics of an EWH are represented through a 10-dimensional state vector, portraying the average temperature of different water stratification layers in the EWH. In this particular case, the heating elements and the temperature sensors are located on the fourth and the ninth layers, respectively. As previously mentioned, the local *MF controller* uses a local vector state feedback law, which needs two pieces of information: (i) the mean temperature of all EWH model strata $T_i, \forall i = 0, \ldots, 9$, and (ii) the boolean value θ, which indicates whether there is water drawn from the tank at a particular instant or not. The objective of the *observer* module is to estimate these values through the readings of two temperature sensors placed near existing heating elements of water heaters (see Figure 4).

Note that a master's thesis [32] was entirely dedicated to the subject of state estimation in EWHs. In this paper, we can only provide a rough idea of the steps involved in the estimation scheme. Let us denote the temperature estimates as $\hat{T}_i$, and the binary hot water demand state estimate as $\hat{\theta}$. We first assume that the statistics of the Markov chain binary state hot water energy extraction process have been identified through an independent process. Then, we describe the estimation algorithm for that discrete state. At the time a new set of measurements becomes available, the two dimensional stream of temperature observations gathered over the past 15 minutes is collapsed into a single mean stream of temperatures *considered as a proxy for the EWH mean temperature* evolution over that period of time. Subsequently, all candidate ON-OFF sequences of water demand exhibiting no more than three switchings over the past 15 minutes are considered, and we only retain those that can account, through the

[5]TRNSYS, "The Transient Energy System Simulation Tool", [Online]. Available: `http://www.trnsys.com/`.

available mathematical model, for the observed sequence of mean temperatures, up to a prespecified maximum level of total square error. This forms a set of binary demand state sequences considered consistent with the observations. Within that set of plausible sequences, the one finally retained as our best estimate is *the one associated with the highest probability of realization*. This permits an estimation of the binary demand process over the past 15 minutes. Given that estimated energy demand process and the sequence of known heating inputs over the past 15 minutes, the temperatures in the various EWH layers are now estimated by running a Kalman filtering algorithm using the available measurements. Further details on the overall estimation scheme can be found in [32].

4.3. Local MF controller: local actions with global results

A significant challenge of a large-scale control of dispersed energy storage in power systems is the presence of literally millions of control points, each contributing a small amount to the overall load and generation smoothing effort. A classical direct control view of this problem, as has been the case in traditional load management programs, would quickly run into the limits of large (and expensive) data communication requirements, and, more importantly, a very large computational burden for the synthesis of the required control signals. Instead, the hybrid control architecture currently adopted enables addressing this issue: it is centralized at the system level for optimal scheduling, as described previously, but decentralized at the implementation level to allow scalability and increase the level of customer acceptance of the controls (since enforcement of security and comfort constraints becomes local). Such an organizing architectural principle is possible thanks to a state-of-the-art development in control theory known as *MF control*. Roughly described, MF control relies on the statistical predictability of large numbers of similar controlled plants or devices to produce optimal controls (i) with significantly reduced communication requirements, and (ii) using distributed computation to apply the required local control signals. Simply put, MF control is the main enabler for smartDESC.

Let us further detail what MF control is and how it can help us in achieving the goal of best steering millions of individual energy storage elements so that their aggregated behavior follows an optimal target trajectory specified at the systems level (further details can be found in [22, 23]). As stated before, a linear dynamics has been adopted for EWHs. A careful choice of a quadratic cost function induces a linear feedback controller, with coefficients calculated backwards in time thanks to so-called Riccati equations. The coefficients are parametrized by θ, a boolean process. The state 0 represents *no water draw* event, whereas 1 represents *water draw*. A scheme of the operation of the local *MF controller* for say EWH_{ij}, i.e. the i^{th} EWH in the j^{th} sub-group, is reported in Figure 5. Note that the *MF controller* receives the 24-hour target profile for the EWH optimal mean temperature of EWHs in the j^{th} subgroup, as computed by the optimization module. It also receives the estimated mean temperature in the j^{th} sub-group at the start of the control horizon. This information is then used by the local *MF controller* to compute a local state feedback law through a fixed-point calculation (see [22] for details). This control law is applied in the feedback loop (see the lower part of Figure 5). The local *MF controller* receives the estimate of the temperature $\hat{T}_i$ of all the layers i in the EWH as well as $\hat{\theta}$. This data is used to set the value of the instantaneous power of the two heating elements of the EWH using an optimal feedback control law. The updated temperature is then captured by the two thermal sensors (i.e., T_3 and T_8). The *observer* employs these two values to update the temperature vector estimates (i.e., $\hat{T}_i$) as well as water draw state estimates (i.e., $\hat{\theta}$). The remarkable fact is that, thanks to the law of large numbers, a locally computed and implemented control law leads at the aggregate level to the mean behavior dictated by the *coordinator*, and thus to a system-wide optimal behavior. Note, however, that for this to happen, the data concerning the EWH physical parameters in homogeneous sub-groups must be regularly updated (for instance, the water inlet temperature changes over the seasons). In addition, the statistical parameters of the water usage statistics must also be updated periodically. These parameter updates can be carried out locally and sent back to the optimization module - at low rates - through the communication module.

5. Simulation results

The smartDESC simulator was developed to design and evaluate load control, renewable penetration and demand response algorithms *in a realistic setting*. The whole environment setup is implemented using Jade (Java Agent Development Framework), which provides a versatile platform for parallel computing. The smartDESC framework provides a layer of abstraction facilitating the design of custom models and provides base classes, conventions and guidelines for their development. It also provides an interface for the user and the environment in which components can run in a coherent manner.

Two simulation scenarios results are presented here. The case presented is based on a population of 400 smartDESC-controlled EWHs, denoted hereafter with s-EWHs, constituting the experimental group. The comparison benchmark is a system of same size, but with traditional t-EWHs, denoted hereafter with t-EWHs, and

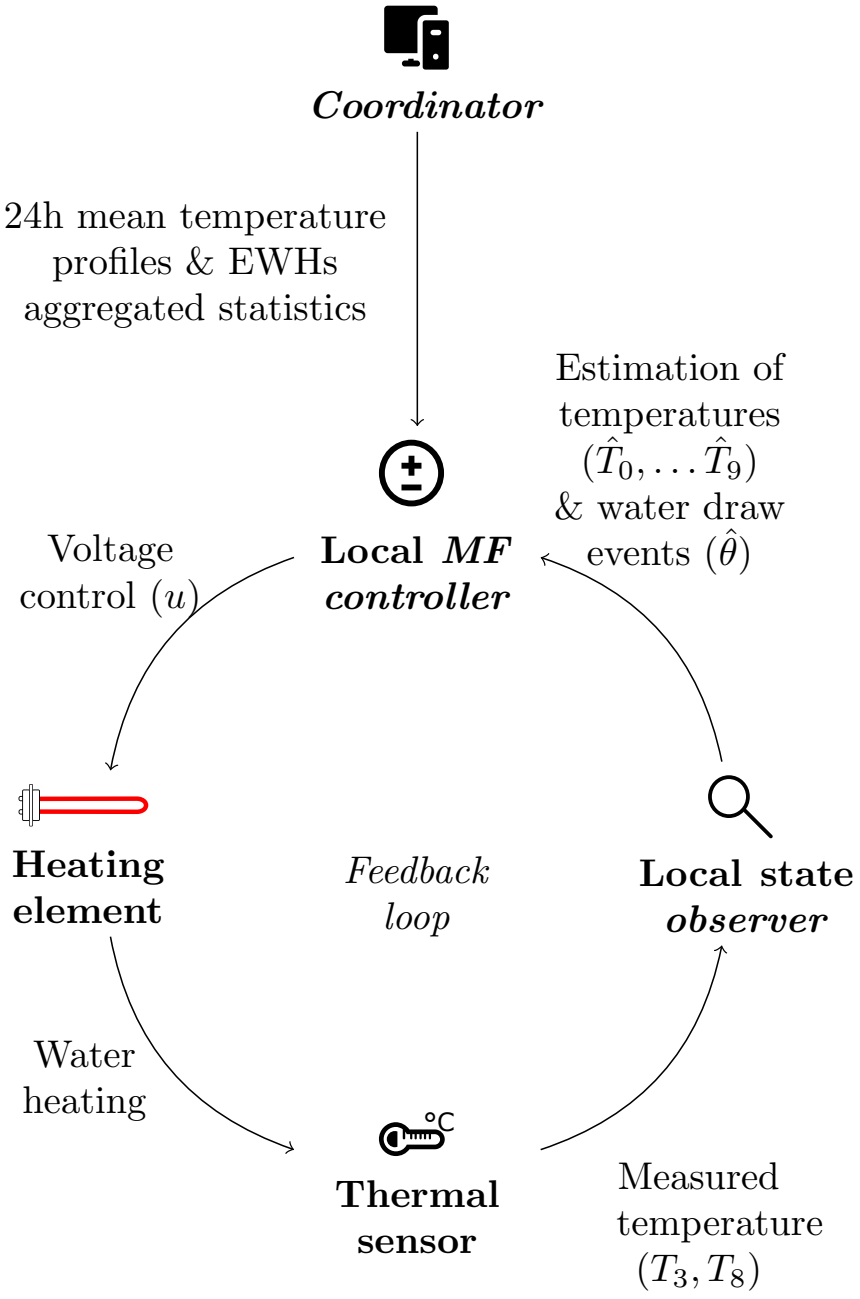

Figure 5: Schematic of the feedback loop in the local *controller*.

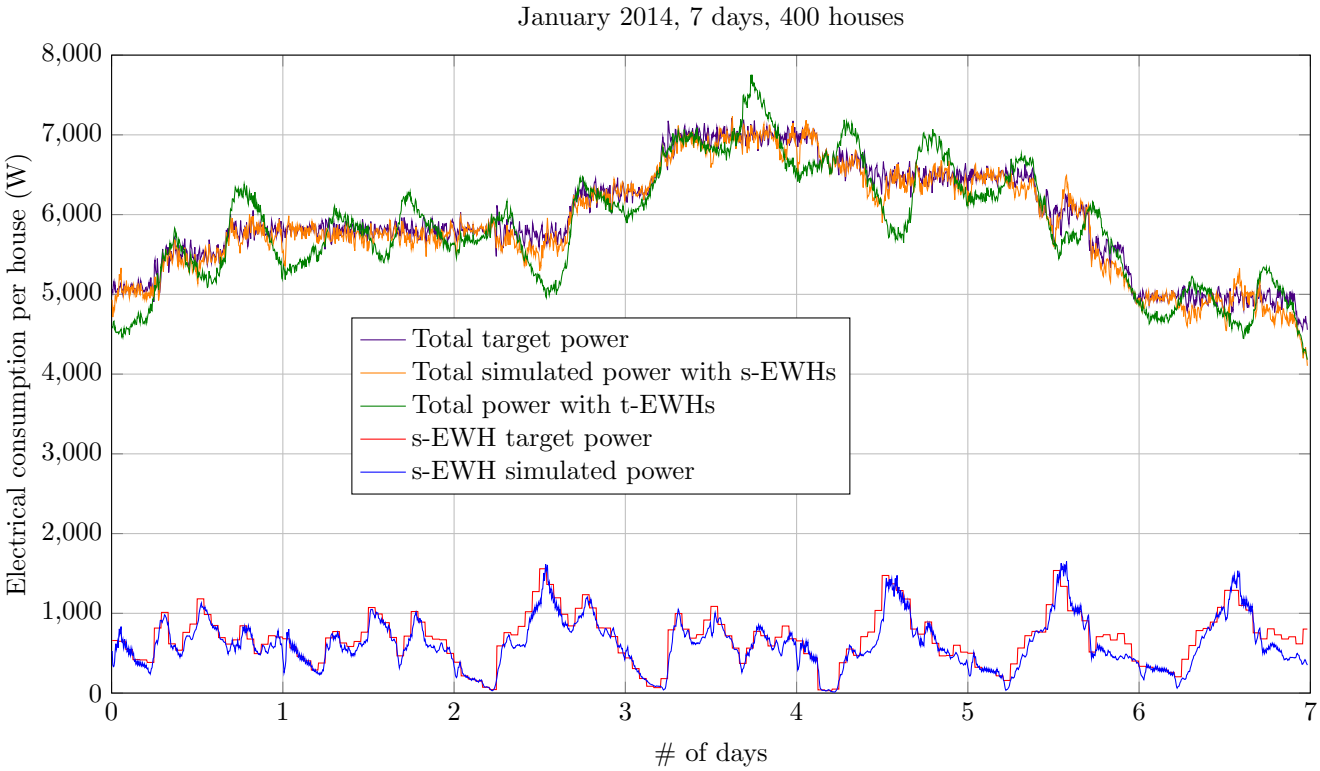

Figure 6: Simulation results with smartDESC controlled EWHs (s-EWHs) as opposed to traditional thermostatically controlled EWHs (t-EWHs) in a deterministic scenario and classical peak shaving objectives.

setpoints at 56°C and 61°C, constituting the control group. These 2 temperatures represent the boundaries of the customer comfort zone: when the temperature is below 56°C a traditional thermostatic controller activates the heating elements, which are subsequently turned off when the temperature reaches 61°C. In order to visualize the full effect of the local smartDESC *MF controllers*, the thermostats have been disabled for the experimental group of s-EWHs: by doing this, the activation of the heating elements is solely decided by local *MF controllers*. Another note is that the *observer* module is also disabled; we basically assume that the exact temperature profile of the tank, and the instantaneous water draw state are available to the *coordinator* at each time instant. This gives a theoretical upper bound on the performance that can be achieved with this approach.

The first simulation result is displayed in Figure 6. At time 0, the optimization module receives the total power consumption (green curve) together with the 7-day power consumption profile (not reported in the figure) for the Thermostatically controlled EWH (t-EWH) population. The uncontrolled load forecast is then computed as the total power consumption minus the t-EWH consumption. The optimization module also calculates the target power profile for s-EWHs, represented with a red curve in the figure. The purple curve represents the total target power, i.e., the uncontrolled load plus the s-EWH target power. smartDESC simulation is then performed and results are also shown in Figure 6: the blue curve represents the power consumption of s-EWHs while the orange curve corresponds to the aggregate power consumption of the whole system.

Simulation results indicate that the mean power profile of the s-EWHs (blue curve) satisfactorily tracks the target (red curve). Comparing the two curves, we computed a root mean square error (RMSE) of 135.279 W with a normalized-RMSE value of 0.088. Consequently, the total simulated power consumption (orange) is close to the target power (purple). The total simulated power curve (orange) also shows a reduced variability and considerable peak shaving, when compared to the total consumed power in the reference scenario where traditional t-EWHs are employed.

In the second simulation, a more complex scenario was considered, assuming the *coordinator* is provided with *random* forecasts of wind production and of uncontrolled electric load demand. Wind production forecasts were generated by the company WPred, based on weather forecasts provided by Environment Canada. The forecast includes the speed and direction of wind between 10 and 150 metres above ground level, as well as the atmospheric pressure and air temperature. Additional details on the generation of wind power scenarios from numerical weather predictions can be found in [33]. The stochastic scenario also includes the uncontrolled load projection in the desired

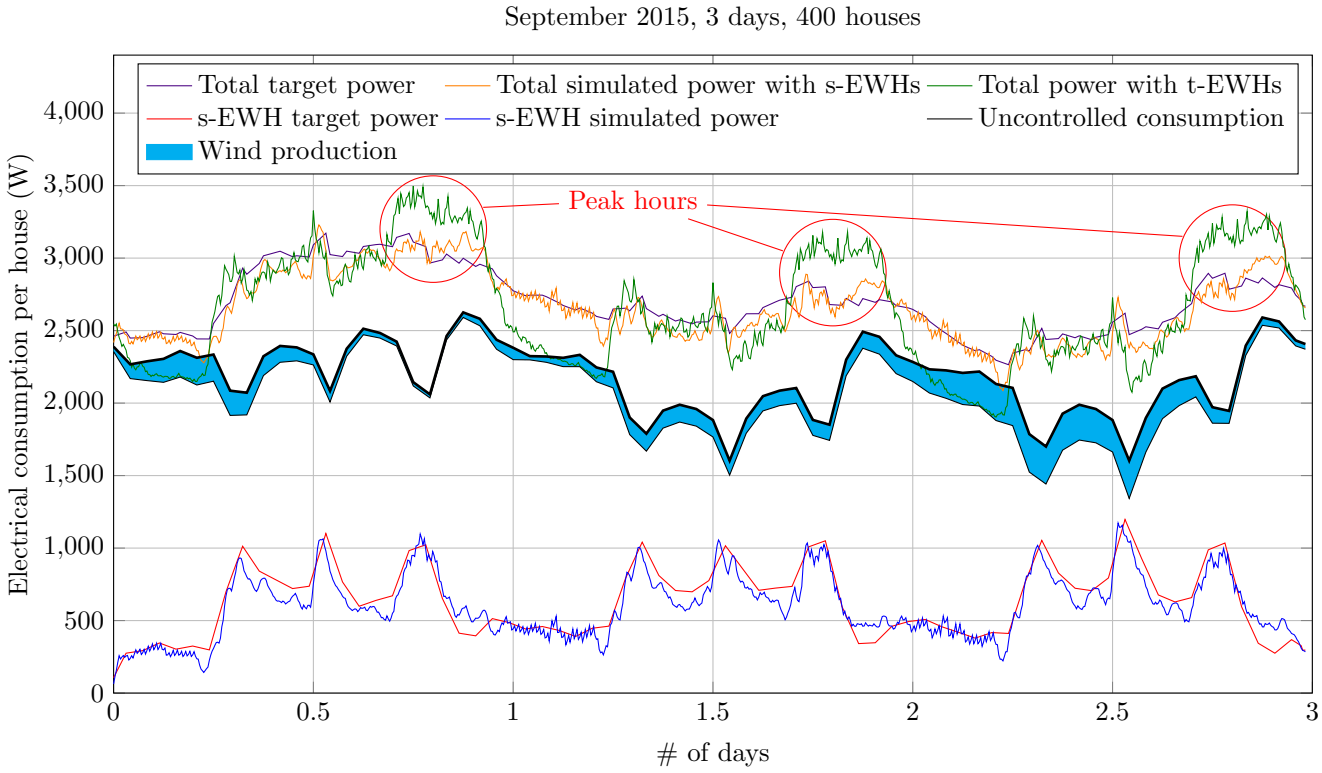

Figure 7: Simulation results with smartDESC controlled EWHs (s-EWHs) as opposed to traditional thermostatically controlled EWHs (t-EWHs) in a more complex scenario with forecasts on wind production; peak hours are circled in red.

time horizon. The load projection module, provided by the company Artelys, is based on the weather forecast and on historical electric load data. Additional details can be found in [34].

The simulation results in the stochastic scenario are displayed in Figure 7. In this figure, the upper border of the cyan area represents the uncontrolled demand, whereas the cyan area itself shows the potential time-varying range of wind power produced. The bottom border of the cyan area represents the net uncontrolled demand. Given the forecast, the *coordinator* computes a target profile for the s-EWH population (red curve). Summing up the uncontrolled demand with the s-EWH target power, one obtains the purple curve, representing the total target power. The green curve represents, as in the previous case, the total consumed power when regular t-EWHs are employed. The behavior of s-EWHs is subsequently simulated: the blue curve represents the simulated power consumption of the 400 s-EWHs and the orange curve represents the total simulated power. The s-EWH power consumption closely follows the target consumption dictated by the *optimization* sub-module of the coordinator (see Section 2 for details). Here the curve comparison gave an RMSE of 91.192 W and a normalized-RMSE value of 0.084. Load balancing characteristic of the orange curve can easily be seen in the figure, in comparison with the green curve. Of particular interest is the valley in the early parts of day 2, where most of the valley filling is due to the peak of wind production.

In order to highlight and quantify the benefit brought by the use of s-EWHs, we analyzed the power reduction in the time interval from 4:30 pm to 10:50 pm in the three days (red-circled in Figure 7): results from this analysis are shown in Table 1. A daily mean reduction in the electrical consumption per house of 236.97 W is observed in those time intervals, which corresponds to 7.68 % of the total consumed power per house when regular t-EWHs are employed. During the peak hours, an average daily energy saving of 1.55 kWh per house was observed. The power consumption reduction was specifically analyzed during peak hours because it is the most difficult to manage by the power operators. The achieved peak-shaving in the average power consumption per house can easily be translated into an overall reduction of the demand during peak hours, with potentially significant value for power operators and even consumers if the electricity cost is higher during these periods.

After having shown the positive effects of using s-EWHs on the aggregated behavior of the system, we now focus on population dynamics. Figure 8 shows how the temperature profile of s-EWHs evolves in time. It is seen that the system maintains variability in temperature at all times but the transitions are smooth. The absence of sudden changes in the temperature distribution is important because it shows that the use of *MF*-based control does not

	Day 1	Day 2	Day 3	Daily mean
Average power reduction (W)	216.55	247.95	246.41	**236.97**
Percentage of power reduction (%)	6.61	8.38	8.17	**7.68**
Energy savings (kWh)	1.41	1.62	1.61	**1.55**

Table 1: Summary of the benefits during peak hours highlighted in Figure 7.

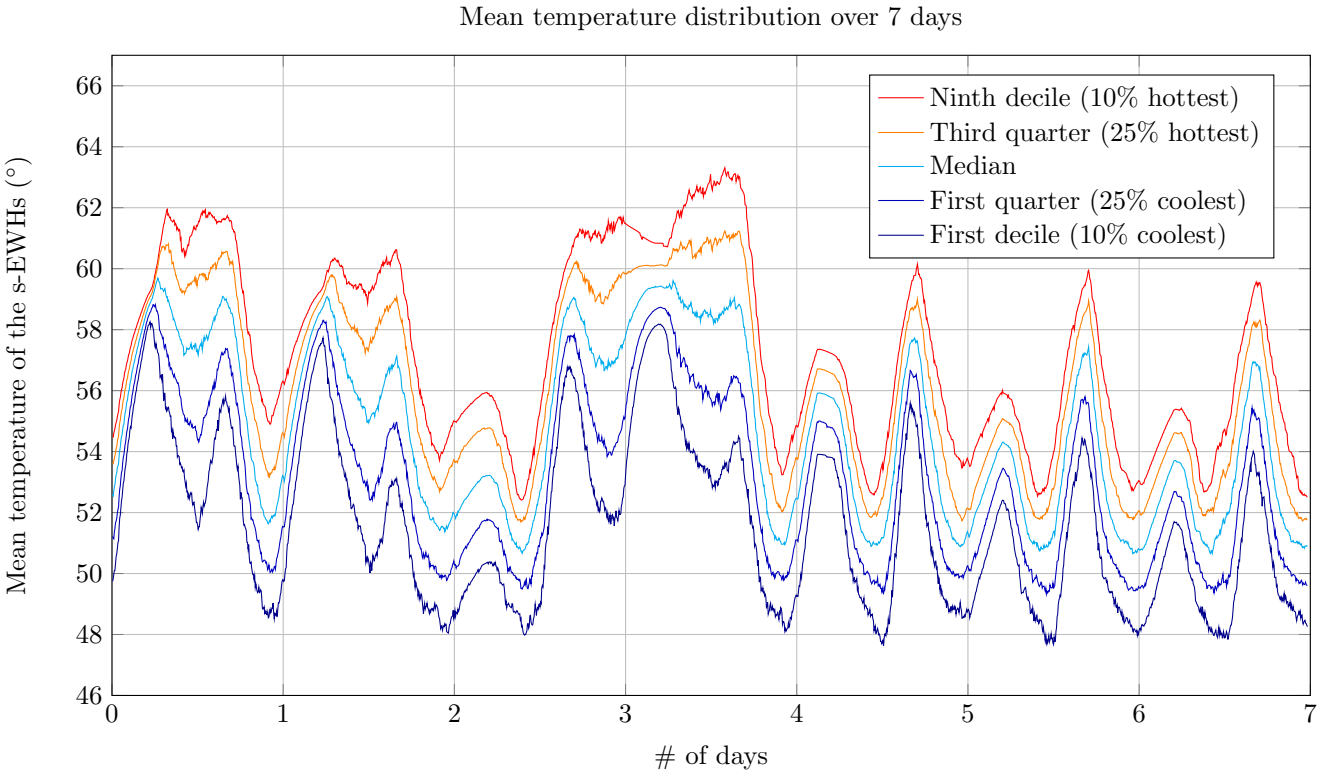

Figure 8: Percentile evolution of the mean temperature of the s-EWHs.

cause steep changes in the tank mean temperature, which would constitute an undesirable situation. Fairness is also important: one of the objectives of the control architecture is that the burden of lowered or increased mean temperature should be evenly distributed across the population. In order to put the fairness characteristic of the control algorithm to test, we report in Figure 9 the temperature curves of three randomly selected s-EWHs (orange, green and purple curves). The orange and blue curves represent the top and bottom deciles, respectively. One can see that individuals switch position quite often. We did not observe unfortunate scenarios with some s-EWHs predominantly within the cold temperature or some others always within the hot temperature zone. These two scenarios would cause the undesirable consequences of a reduction of customer comfort or a higher cost of heating, respectively.

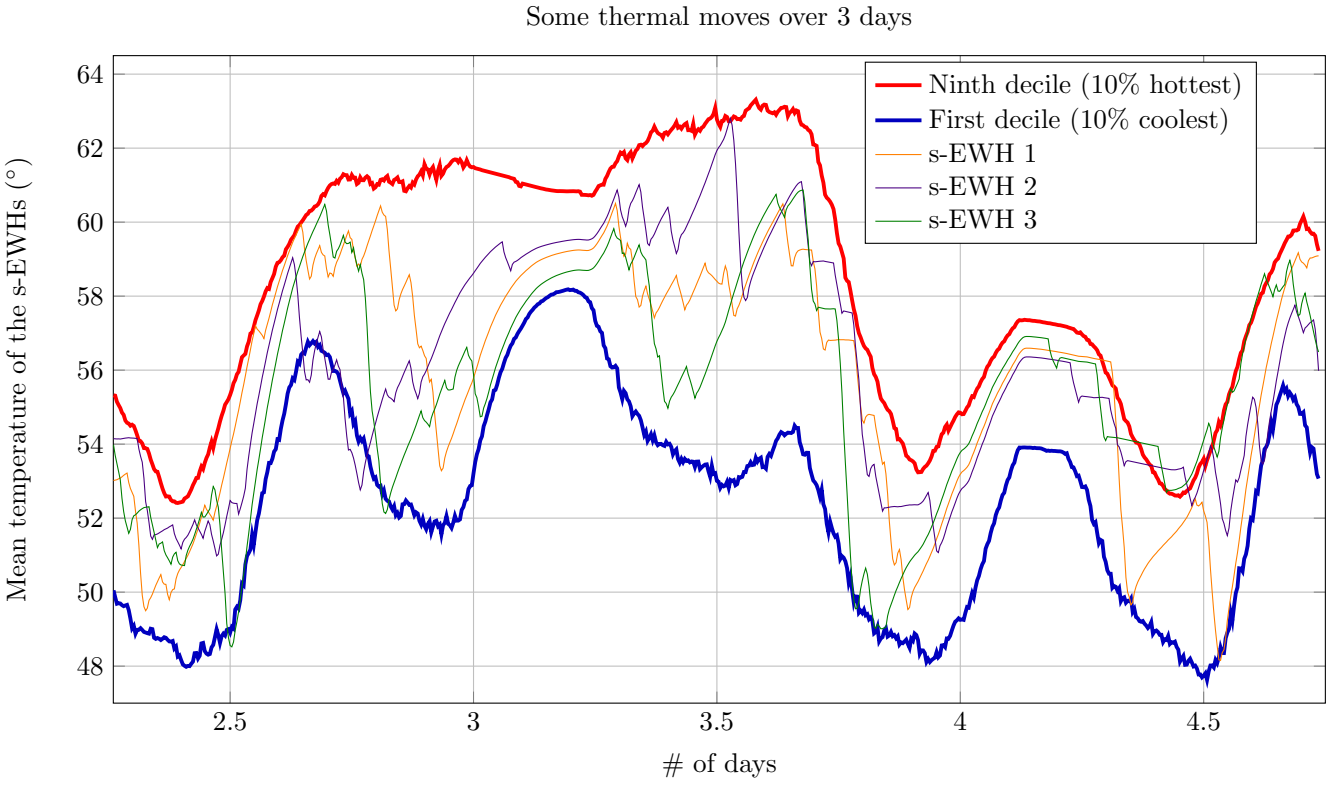

Figure 9: Temperature profile of three s-EWHs and percentile evolution.

In terms of communications, numerical results show the delay in the downlink direction to be significantly higher than the uplink delay. This is because the transmission times of uplink packets, randomly generated by each local *MF controller*, are usually well spread over time. On the other hand, the *coordinator* transmits the same target temperature to all the local *MF controllers* at the same time, in a broadcast fashion. This mechanism causes network congestion, mainly due to the limited size of node buffers. Moreover, the required utilization of the communication channels is very low (the smart meters transmit packets only about 0.13% of the time on average).

6. Conclusions

The smartDESC concept offers an integrated architecture to turn the energy storage potential of distributed existing electrical devices into a reliable and responsive asset for load and generation leveling. The foundation of smartDESC lays in a recent theoretical development, i.e., *mean field* control theory, which is used to manage the macro-micro separation of optimization at the utility level and control at the local level. It constitutes a novel paradigm that could find applications in many different areas of engineering. The smartDESC architecture has been implemented in a simulator and tested on realistic case studies involving a homogeneous population of electric water heaters (EWHs) in a grid with renewable penetration. The simulation results showed that the smartDESC approach reduces the burden to power operators during peak hours with minimal impact on the comfort of customers. The simulation scenario with realistic wind power generation showed that the use of smartDESC-controlled EWHs could

enable a more efficient use of power coming from renewable sources. Overall, the results showed that the smartDESC concept works as expected, and no substantial issue of scalability is expected to arise.

It is worth mentioning that a hardware implementation of a local *mean field controller* was realized and installed on a real EWH, which has been tested jointly with the simulated EWHs (not shown in this paper): the concept also proved to work on the physical device. The smartDESC concept is therefore ready to progress towards a hardware testing stage. More details about the smartDESC project can be found in the public report available online [34].

Acknowledgments

This project was primarily funded by the Canadian federal government's ecoENERGY Innovation Initiative (ecoEII), between 2012 and 2016 (project RENE-034). The authors gratefully acknowledge this financial contribution, as well as the in-kind contributions of many other partners, namely: Laboratoire des Technologies de l'Énergie (LTE) of IREQ (Institut de Recherche d'Hydro-Québec), WPred Inc., Artelys, SG2B, and Coopérative St-Jean-Baptiste (a small electricity distributor in Montérégie, QC, Canada). The authors also address a special thanks to all researchers and students who took part in this project, namely (in alphabetical order): D. Beauvais, B. Bourdel, J. Coulombe, S. Fan, F. Li, R. Losseau, K. Ratelle, M. Sauvé, J. Solis and A. I. Tammam.

References

For Further Reading

[1] L. Hughes, "Meeting residential space heating demand with wind-generated electricity," *Renewable Energy*, vol. 35, no. 8, pp. 1765–1772, 2010.

[2] B. M. Mitchell, W. G. Manning, and J. P. Acton, *Electricity pricing and load management: Foreign experience and California opportunities*. Rand, 1977.

[3] X. Xu, C.-f. Chen, X. Zhu, and Q. Hu, "Promoting acceptance of direct load control programs in the united states: Financial incentive versus control option," *Energy*, vol. 147, pp. 1278–1287, 2018.

[4] California Energy Commission *et al.*, "California renewable energy overview and programs," *California Energy Commission. Accessed February 18th*, 2013.

[5] N. Johnson and D. Kennis, "Feed-in tariffs for solar powered cities," Available at `http://www.worldwatch.org/node/5430`.

[6] J. Gillis, "A tricky transition from fossil fuel: Denmark aims for 100 percent renewable energy," *New York Times*, 2014.

[7] D.-A. Ciupăgeanu, G. Lăzăroiu, and L. Barelli, "Wind energy integration: Variability analysis and power system impact assessment," *Energy*, vol. 185, pp. 1183–1196, 2019.

[8] M. Gilani, A. Kazemi, and M. Ghasemi, "Distribution system resilience enhancement by microgrid formation considering distributed energy resources," *Energy*, vol. 191, pp. 375 – 87, 2020.

[9] H. Cai, A. Thingvad, S. You, and M. Marinelli, "Experimental evaluation of an integrated demand response program using electric heat boosters to provide multi-system services," *Energy*, vol. 193, 2020.

[10] M. McPherson and B. Stoll, "Demand response for variable renewable energy integration: A proposed approach and its impacts," *Energy*, vol. 197, 2020.

[11] L. Hirth and I. Ziegenhagen, "Control power and variable renewables," in *2013 10th International Conference on the European Energy Market (EEM)*, pp. 1–8, IEEE, 2013.

[12] T. Ackermann, E. M. Carlini, B. Ernst, F. Groome, A. Orths, J. O'Sullivan, M. de la Torre Rodriguez, and V. Silva, "Integrating variable renewables in europe: Current status and recent extreme events," *IEEE Power and Energy Magazine*, vol. 13, no. 6, pp. 67–77, 2015.

[13] G. El Rahi, W. Saad, A. Glass, N. B. Mandayam, and H. V. Poor, "Prospect theory for prosumer-centric energy trading in the smart grid," in *2016 IEEE Power & Energy Society Innovative Smart Grid Technologies Conference (ISGT)*, pp. 1–5, IEEE, 2016.

[14] M. Kovač, G. Stegnar, F. Al-Mansour, S. Merše, and A. Pečjak, "Assessing solar potential and battery instalment for self-sufficient buildings with simplified model," *Energy*, vol. 173, pp. 1182–1195, 2019.

[15] H. M. Marczinkowski and P. A. Østergaard, "Residential versus communal combination of photovoltaic and battery in smart energy systems," *Energy*, vol. 152, pp. 466–475, 2018.

[16] H. Mehrjerdi and R. Hemmati, "Energy and uncertainty management through domestic demand response in the residential building," *Energy*, vol. 192, 2020.

[17] A. Bostan, M. S. Nazar, M. Shafie-khah, and J. P. Catalao, "An integrated optimization framework for combined heat and power units, distributed generation and plug-in electric vehicles," *Energy*, vol. 202, 2020.

[18] J. L. Mathieu, M. Kamgarpour, J. Lygeros, and D. S. Callaway, "Energy arbitrage with thermostatically controlled loads," in *2013 European Control Conference (ECC)*, pp. 2519–2526, IEEE, 2013.

[19] E. Vrettos, S. Koch, and G. Andersson, "Load frequency control by aggregations of thermally stratified electric water heaters," in *2012 3rd IEEE PES Innovative Smart Grid Technologies Europe (ISGT Europe)*, pp. 1–8, IEEE, 2012.

[20] S. Meyn, P. Barooah, A. Bušić, and J. Ehren, "Ancillary service to the grid from deferrable loads: The case for intelligent pool pumps in florida," in *52nd IEEE Conference on Decision and Control*, pp. 6946–6953, IEEE, 2013.

[21] Z. Ma, D. S. Callaway, and I. A. Hiskens, "Decentralized charging control of large populations of plug-in electric vehicles," *IEEE Transactions on Control Systems Technology*, vol. 21, no. 1, pp. 67–78, 2013.

[22] A. C. Kizilkale and R. P. Malhamé, "Collective target tracking mean field control for markovian jump-driven models of electric water heating loads," in *Control of Complex Systems*, pp. 559–584, Elsevier, 2016.

[23] A. C. Kizilkale, R. Salhab, and R. P. Malhamé, "An integral control formulation of mean field game based large scale coordination of loads in smart grids," *Automatica*, vol. 100, pp. 312–322, 2019.

[24] R. Losseau, "Modélisation agrégée de chauffe-eau électrique commandé par champ moyen pour la géstion des charges dans un réseau," Master's thesis, École Polytechnique de Montréal, 2016. Available at `https://publications.polymtl.ca/2175/`.

[25] A. I. Tammam, *Lissage optimal de la charge électrique en présence de sources d'énergies renouvelables via le pilotage de la consommation des chauffe-eau*. PhD thesis, École Polytechnique de Montréal, 2016. Available at `https://publications.polymtl.ca/2254/`.

[26] A. I. Tammam, M. F. Anjos, and M. Gendreau, "Balancing supply and demand in the presence of renewable generation via demand response for electric water heaters," *Annals of Operations Research*, 2020. Available at `https://doi.org/10.1007/s10479-020-03580-1`.

[27] F. Malandra and B. Sansò, "A simulation framework for network performance evaluation of large-scale RF-mesh AMIs," *Simulation Modelling Practice and Theory*, vol. 75, pp. 165 – 181, 2017.

[28] F. Malandra, *A Framework for the Performance Analysis and Simulation of RF-Mesh Advanced Metering Infrastructures for Smart Grid Applications*. PhD thesis, École Polytechnique de Montréal, 2016. Available at `https://publications.polymtl.ca/2422/`.

[29] F. Malandra and B. Sansò, "Analytical performance analysis of a large-scale RF-Mesh smart meter communication system," in *2015 IEEE Power Energy Society Innovative Smart Grid Technologies Conference (ISGT)*, pp. 1–5, IEEE, Nov. 2015.

[30] F. Malandra and B. Sansò, "PeRF-Mesh: A performance analysis tool for large scale RF-Mesh-based smart meter networks with FHSS," in *2015 IEEE International Conference on Smart Grid Communications (SmartGridComm)*, pp. 792–797, IEEE, 2015.

[31] J. Laurent and R. Malhamé, "A physically-based computer model of aggregate electric water heating loads," *IEEE transactions on power systems*, vol. 9, no. 3, pp. 1209–1217, 1994.

[32] J. Solis, "Développement d'un estimateur d'état énergétique d'un chauffe-eau pour un contrôle par champ moyen," Master's thesis, École Polytechnique de Montréal, 2015. Available at `https://publications.polymtl.ca/2014/`.

[33] A.I. Tammam, C.S. Watters, M.F. Anjos, and M. Gendreau, "A methodology for ensemble wind power scenarios generation from numerical weather predictions," in *2016 IEEE Power and Energy Society General Meeting (PESGM)*, pp. 1–5, July 2016.

[34] F. Sirois, B. Bourdel, and R. P. Malhamé, *Management of distributed energy storage capacity scattered in electric power systems for damping the variability of renewable energy sources – Public Report for project RENE-034*. Natural Resources Canada, July 2017. Available at `https://www.nrcan.gc.ca/energy/funding/current-funding-programs/eii/16102`.